POST-CRACKING BEHAVIOUR OF SELFCOMPACTING STEEL FIBRE REINFORCED CONCRETE

E. N. B. Pereira, J. A. O. Barros, A. F. Ribeiro, A. Camões
University of Minho, Portugal

Abstract

Self-compacting concrete (SCC) can be defined as concrete that is able to flow in the interior of the formwork, passing through the reinforcement and filling it in a natural manner, being consolidated under the action of its own weight. Adding the benefits of SCC to those resulting from the addition of discrete fibres to cement based materials, a high performance material, designated by steel fibre reinforced self-compacting concrete (SFRSCC), is obtained. In the present work the strategy followed to design SFRSCC is described, as well as, the experimental research carried out to characterize its flexural and compression behaviour. A special effort is done to assess the post-cracking behaviour, carrying out three point notched beam tests. The equivalent and the residual flexural tensile strength parameters, proposed by RILEM TC 162-TDF to characterize the toughness of steel fibre reinforced concrete (SFRC), are determined. To evaluate the stress-crack opening diagram of the designed SFRSCC, an inverse analysis is performed fitting the obtained experimental force-deflection curves.

1. Introduction

The concrete precasting industry is frequently confronted with the production of structural reinforced concrete elements of some geometric complexity. These structures, sometimes, include very thin elements and curved components. These geometric conditions introduce difficulties on the placement of the reinforcement, resulting in a large consuming time phase of the industrial process. Moreover, when high percentage of reinforcement is used, there are difficulties on assuring the desired concrete pouring quality, resulting deficiencies that can compromise the mechanical behaviour and the visual appearance of the final structure.

The use of self-compacting concrete (SCC) can overcome the obstacles resulting from the geometric complexity of the structure, as well as, the passing and flowing restrictions introduced by high percentage of reinforcement. Adding steel fibres to SCC, part of the conventional reinforcement (bars and wire-meshes) can be suppressed, decreasing the obstacles of assuring high concrete pouring quality. There are, even, structures of high degree of hyperstaticity, like slabs supported on soil and underground structures, in which almost conventional reinforcement can be replaced by steel fibres, with technical and economical advantages.

In the fresh state, concrete can be considered as a two-phase material: the solid phase includes aggregate particles of equivalent diameter greater than 150 µm; the fluid phase

Eduardo Pereira, Post cracking of selfcompacting steel, 1/10
Fax: +351 253510217
E-mail: .epereira@civil.uminho.pt

consists of a suspension of fine particles (equivalent diameter <150μm), water, superplasticizer, viscosity and air entraining agents that fulfil the empty spaces in-between the particles of the solid phase. The main target in solid phase is to obtain the most compact solid skeleton [1, 2]. In the present work, this strategy was used on the development of the steel fibre reinforced self compacting concrete (SFRSCC), since it reduces the void index, resulting advantages both in terms of strength and ability to flow. When using the proposed method, the influence of the fibres in the skeleton organisation is directly assessed. To optimize the fluid phase (binder paste) simple test methods, like the "Marsh cone" and the "Flow table" were used in the present work, since more sophisticated tests require expensive equipments, like last generation of rheometers, that are not available in the majority of the laboratories and are not adjusted for field applications.

The present work is part of a research program for the development of lightweight sandwich SFRSCC panels for precasting industry. The SFRSCC to develop should have the following mechanical properties: average compression strength at seven days greater than 50 MPa and equivalent flexural tensile strength greater than 3 MPa at this age [1]. Due to economical reasons, these values should be attained with a cement content not exceeding 410 Kg/m^3 and without the use of silica fume. To simulate the post-cracking behaviour of SFRSCC structure the fracture parameters of this composite should be known. For this purpose, an inverse analysis was carried out using the force-deflection relationships obtained in the flexural tests and a finite element computational code.

2. Rational method for conceiving SFRSCC

The materials used were cement (C) CEM I 42.5R, fly ash (FA), limestone filler (LF), superplasticizer (SP) of third generation based on polycarboxilates (Glenium® 77SCC), water (W), three types of aggregates (fine river sand, coarse river sand and crushed granite 5-12 mm) and DRAMIX® RC-80/60-BN steel fibres. This fibre has a length (l_f) of 60 mm, a diameter (d_f) of 0.75 mm, an aspect ratio (l_f/d_f) of 80 and a yield stress of 1100 MPa. The method developed in the present work is based on the three following steps: i) the proportions of the constituent materials of the binder paste are defined; ii) the proportions of each aggregate on the final solid skeleton are determined; iii) binder paste and solid skeleton are mixed in different proportions until selfcompacting requirements in terms of spread ability, correct flow velocity, filling ability, blockage and segregation resistance are assured.

2.1 Binder paste composition
In this first step, a series of tests were performed to achieve the optimum composition of the binder paste. To define the optimum percentage of FA addition in the final composition, several mixes of FA, cement and water were executed. The proportions of each component were defined in terms of volume, and the percentage in volume of FA has varied between 0% and 50% of the cement volume. To promote the dispersion and deflocculation of the fine particles in suspension [3], a small constant quantity of

Eduardo Pereira, Post cracking of selfcompacting steel, 2/10
Fax: +351 253510217
E-mail: .epereira@civil.uminho.pt

superplasticizer was also added to each mix. The relative spread of each mix was measured and the results are depicted in Fig. 1.
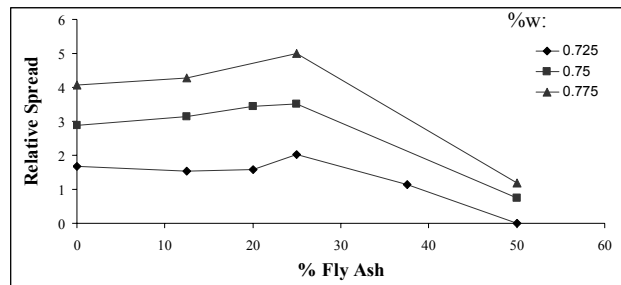

Fig. 1 - Optimization of the percentage of Fly Ash

The shape of the curves obtained for the three analysed water content (in volume of the fine material – C+FA+LF) show, first of all, that the optimum percentage of FA is about 25%, and secondly, that the optimum value doesn't seem to depend on water content.

Keeping constant the percentage of FA (25% of the volume of cement), a new series of mixes was done adding limestone filler in a proportion between 0% and 125% of the cement volume. A quantity of $0.035 dm^3$ of SP per dm^3 of fine material was added to each mix. The relative spread achieved in the "Flow table" and the "Marsh cone" flow time of each mix were measured. To give some guidance in the paste phase design, the compression strength of each mix was also evaluated on 5 cm edge cubic specimens at an age of 7 days. The results are represented in Fig. 2.

Figs. 2a and 2b show that, increasing the percentage of LF, the flowing time reduces and the relative spread increases. The shape of the curves, once more, is independent of the water percentage. It seems, however, that the increase of LF beyond 50% is not so profitable. Fig. 2c reveals that increasing the percentage of LF the compression strength reduces, and this tendency seems to be stronger for percentages of LF higher than 50%. Taking into account all these aspects, the optimum percentage of LF can reasonably be fixed at 50%.

Up to this step, the content of superplasticizer was kept constant in every mixes. To optimize its value, some pastes with distinct percentages of superplasticizer were produced, keeping constant all the other components already optimized. For each paste, the "Flow table" relative spread, the "Marsh cone" flowing time and the compression strength (cubes of 5 cm at 7 days old) were measured. The obtained results are indicated in Fig. 4.
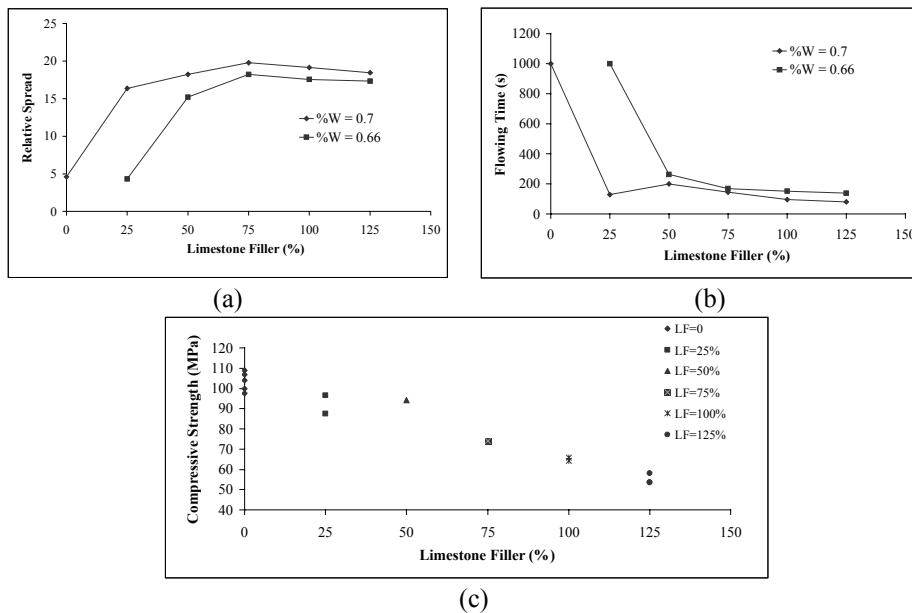
Eduardo Pereira, Post cracking of selfcompacting steel, 3/10
Fax: +351 253510217
E-mail: .epereira@civil.uminho.pt

(a)

(b)

(c)

Fig. 2 - Influence of the LF on the relative spread (a), flow time (b) and compression strength (c).

According to Fig. 3b, the mix with 0,035dm^3 of superplasticizer per dm^3 of fine materials (C+FA+LF) had the highest compression strength. Fig. 3a reveals that the "Marsh cone" flowing time and the "Flow table" relative spread are not significantly affected when increasing the SP content beyond 0.035 dm^3 per dm^3 of fine material. Therefore, this value was assumed as being the optimum amount of SP.
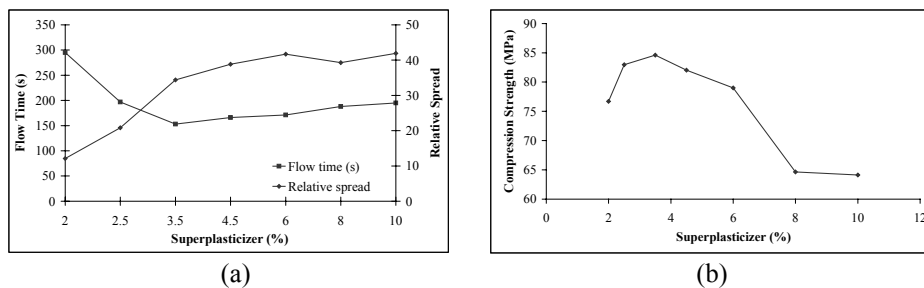

(a)

(b)

Fig. 3 - Influence of the percentage of SP on the flow time (a), and on the compression strength (b).

2.2 - Solid skeleton composition

To define the most appropriate proportions of the three types of aggregates, some mixes were made with different quantities of each type of aggregate, and the weight of a 5 dm^3

Eduardo Pereira, Post cracking of selfcompacting steel, 4/10
Fax: +351 253510217
E-mail: .epereira@civil.uminho.pt

volume of each mix was measured. The optimum aggregate mix was assumed as being the heaviest one, since it should correspond to the most compact. An estimated portion of fibres equivalent to 30 Kg of fibres per m^3 of concrete was included in every mixture. Initially, only two of the three types of aggregates were mixed. Some compositions of crushed stone and coarse sand in different proportions were then made, and the weight of a 5 dm^3 volume of each one was measured. The line with diamond marks included in Fig. 4 represents the obtained results. The maximum point in this curve corresponds to the heaviest mix, or in other words, to the most compact one. These results indicate that the optimum composition of the solid skeleton should be composed, in volume, by 55% of coarse sand and 45% of crushed stone.

Attempting to increase the solid skeleton compacity, another group of mixes was made. Relative percentage of coarse sand and crushed stone was maintained constant, while the percentage, in volume, of the fine sand was varied. The line with circle markers depicted in Fig. 4 represents the obtained results, from which an optimum percentage of fine sand of 10% of the total volume of aggregates was determined.
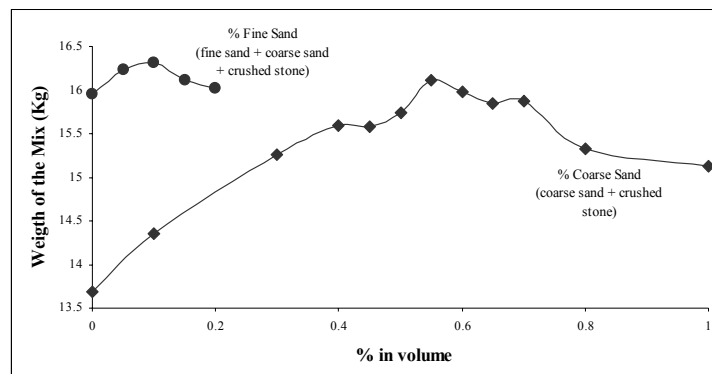

Fig. 4 - Optimisation procedure of the aggregate skeleton

2.3- Paste content in the final composition

This phase is dedicated to the evaluation of the paste content in the concrete volume. The optimum composition would accomplish an upper limit around 400 Kg per cubic meter of concrete imposed for the cement content. To achieve the optimum paste content, some mixes of concrete were conceived, varying the paste percentage. For each mix, the added water was evaluated taking into account the aggregate's saturation degree. The mix process was always the same, and for each mix the slump flow test was executed. Total spread, s, and time to reach a spread diameter of 500 mm, T_{50}, were measured. Table 1 includes the composition that best fit selfcompacting requirements.

No sign of segregation was detected, a total spread of 775 mm was measured and the mixture showed good homogeneity and cohesion, even when flowing trough the small orifice of the Abrams cone (when testing, Abrams cone was always used in the inverted position). A T_{50} of 4.6 seconds was measured.

Eduardo Pereira, Post cracking of selfcompacting steel, 5/10
Fax: +351 253510217
E-mail: .epereira@civil.uminho.pt

Table 1 - Final composition for 1m³ of SFRSCC made with 30 Kg/m³ of fibres

Paste/Total volume (%)	Cement (Kg)	FA (Kg)	Water (Kg)	SP (dm³)	LF (Kg)	Fine sand (Kg)	Coarse sand (Kg)	Crushed aggregates (Kg)
0.34	408.00	76.50	97.35	8.05	183.94	123.82	753.33	675.47

3. Mechanical Properties

3.1. Compression

To assess the uniaxial compression behaviour of seven days SFRSCC, ten cylinder specimens of 150 mm diameter and 300 mm height were tested under displacement control. Average compression strength of 56.45 MPa was obtained with a standard deviation of 2.5 MPa. For a cement content of 408 kg/m³ and for SFRSCC of seven days old, this compression strength level is quite high [4], and is enough for the majority of the structural applications.

3.2. Flexural

To assess the flexural behaviour of the SFRSCC, the specimen geometry (600×150×150 mm³), the curing procedures, the position and dimensions of the notch sawn into the specimen, the loading and specimen support conditions, the characteristics for both the equipment and measuring devices, and the test procedures recommended by RILEM TC 162-TDF [5] were adopted. The method for casting the specimens proposed by RILEM TC 162-TDF was adapted for SFRSCC since the specimens were moulded without any external compaction energy. Fig. 5a represents the force-deflection curves, F-δ, obtained in the eight tested specimens. The envelope and the average F-δ curves are depicted in Fig. 5b.
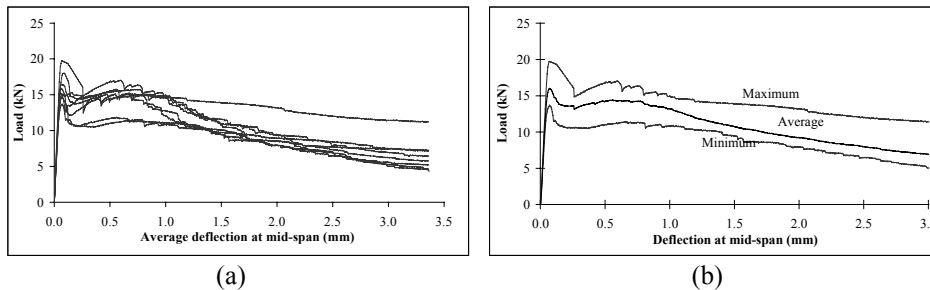

(a)   (b)

Fig. 5 - Force-deflection curves obtained in the three point bending notched SFRSCC beam tests (a) and their corresponding envelope and average curves (b)

Using the F-δ relationships, RILEM TC 162-TDF proposed the evaluation of the load at the limit of proportionality (F_L), the equivalent ($f_{eq,2}$ and $f_{eq,3}$) and the residual ($f_{R,1}$ and $f_{R,4}$) flexural tensile strength parameters [5, 6]. F_L is the highest value of the load

Eduardo Pereira, Post cracking of selfcompacting steel, 6/10
Fax: +351 253510217
E-mail: .epereira@civil.uminho.pt

recorded up to a deflection (or CMOD) of 0.05 mm. The parameters $f_{eq,2}$ and $f_{eq,3}$ are related to the material energy absorption capacity up to a deflection of δ_2 and δ_3 ($\delta_2 = \delta_L + 0.65$ mm and $\delta_3 = \delta_L + 2.65$ mm, where δ_L is the deflection corresponding to F_L) provided by fibre reinforcement mechanisms ($D^f_{BZ,2}$ and $D^f_{BZ,3}$), as seen in Figs. 6 and 7. The parcel of the energy due to matrix cracking (D^b_{BZ}) is not considered in the f_{eq} evaluation. The parameters $f_{R,1}$ and $f_{R,4}$ are the stresses for the forces $F_{R,1}$ and $F_{R,4}$, respectively, at deflection of $\delta_{R,1} = 0.46$ mm and $\delta_{R,4} = 3.0$ mm. According to RILEM TC 162-TDF, the equivalent and the residual flexural tensile strength parameters are obtained from the following expressions [5, 6]:

$$f_{eq,2} = \frac{3}{2} \frac{D^f_{BZ,2}}{0.50} \frac{L}{bh^2_{sp}} \ [\text{N/mm}^2] \qquad f_{eq,3} = \frac{3}{2} \frac{D^f_{BZ,3}}{2.50} \frac{L}{bh^2_{sp}} \ [\text{N/mm}^2] \qquad (1)$$

$$f_{R,1} = \frac{3}{2} \frac{F_{R,1}L}{bh^2_{sp}} \ [\text{N/mm}^2] \qquad f_{R,4} = \frac{3}{2} \frac{F_{R,4}L}{bh^2_{sp}} \ [\text{N/mm}^2] \qquad (2)$$

where b (=150 mm) and L (=500 mm) are the width and the span of the specimen, and h_{sp} (=125 mm) is the distance between the tip of the notch and the top of the cross section.
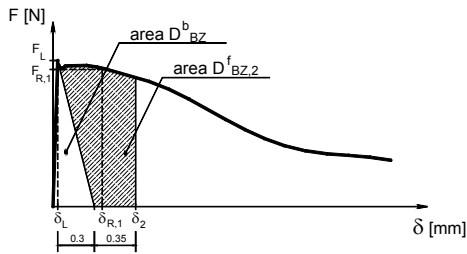

Fig. 6 - Evaluation of $f_{eq,2}$ and $f_{R,1}$ flexural tensile strength parameters according to RILEM TC 162-TDF [5, 6].
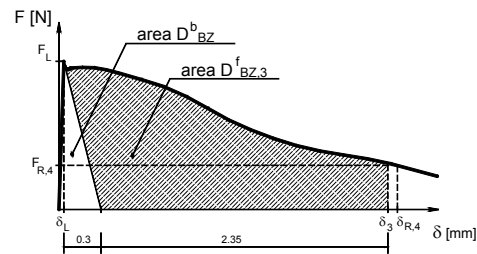
Fig. 7 - Evaluation of $f_{eq,3}$ and $f_{R,4}$ flexural tensile strength parameters according to RILEM TC 162-TDF [5, 6].

From the F-δ relationships obtained in the SFRSCC tested specimens, the values included in Table 2 were determined. In this table $f_{fct,L}$ is the stress corresponding to force F_L and $E_{c,f}$ is the concrete elasticity modulus evaluated from the approach proposed by Petersson [7].

Table 2 - Main data obtained from the three point bending notched SFRSCC beam tests

	$f_{fct,L}$ (MPa)	$E_{c,f}$ (GPa)	$f_{eq,2}$ (MPa)	$f_{eq,3}$ (MPa)	$f_{R,1}$ (MPa)	$f_{R,4}$ (MPa)
Mean value	4.78	32.53	4.30	3.51	4.53	2.22
Std. Deviation	0.52	3.25	0.63	0.44	0.62	0.66
Coef. Correlation (%)	10.83	9.99	14.66	12.53	13.66	29.64

Eduardo Pereira, Post cracking of selfcompacting steel, 7/10
Fax: +351 253510217
E-mail: .epereira@civil.uminho.pt

Using the results obtained from uniaxial compression tests and the recommendations of CEB-FIP 1993 [8], values of 4.0 MPa, 6.3 MPa and 38.28 GPa are obtained for the average axial tensile strength, $f_{fctm,ax}$, average flexural tensile strength, $f_{fctm,fl}$, and tangent Young's Modulus, E_{ci}, respectively (the notch sensitivity was not taken into account in the evaluation of these values). The $f_{fct,L}$ is larger than $f_{fctm,ax}$, since cracking occurred before the force F_L has been attained. The $f_{fct,L}$ is lower than $f_{fctm,fl}$ since in the tested specimens the maximum load, F_{max}, was attained for a deflection greater than the δ_L, i.e., in these cases the F_{max} values were greater than the F_L values. For the specimens used and for the tested SFRSCC, the approach proposed by Petersson leads to elasticity module values lower than the E_{ci} value.

4. Stress-crack opening relationship

4.1. Numerical strategy

To assess the stress-crack opening relationship ($\sigma - w$) of the conceived SFRSCC, an inverse analysis was performed, evaluating the values of the σ_i and w_i of the trilinear $\sigma - w$ diagram (see Fig. 8) that best fit the experimental $F - \delta$ curves with the minimum error of the parameter

$$err = \left| A_{F-\delta}^{\exp} - A_{F-\delta}^{num} \right| \bigg/ A_{F-\delta}^{\exp} \qquad (3)$$

where $A_{F-\delta}^{\exp}$ and $A_{F-\delta}^{num}$ are the areas below the experimental and the numerical $F - \delta$ curves, respectively.

Six-node 2D line interface finite elements were located in the specimen's symmetry axis to model the crack initiation and crack propagation [9]. In the remaining parts of the specimen, linear eight-node Serendipity plane-stress elements were used. In the present analysis the computational code named FEMIX was used [10]. Gauss-Lobatto integration scheme [11] with three integration points (IP) was used for the 2D line interface finite elements, while Gauss-Legendre integration scheme with 2×2 IP was used for the eight-node elements. To avoid undesired spurious oscillations of the stress field, a value of 1.0×10^4 N/mm^3 was assigned to the initial mode I stiffness for the interface element [11]. Since in this problem sliding does not occur in the interface elements, the analysis is independent of the values assigned to the mode II stiffness of the interface element. The value of E_c considered in each numerical analysis was the one that has best fit the experimental $F - \delta$ curve up to crack initiation.

The adequacy of the numerical strategy adopted is shown in Fig. 9, revealing that the proposed trilinear $\sigma - w$ diagram is capable of predicting, with enough accuracy, the post-cracking behaviour of the tested specimens. The experimental $F - \delta$ curve is the average of the overall responses obtained from the tested specimens. The values for σ_i and w_i are included in Table 3 and correspond to the simulation of the average $F - \delta$ experimental curve. The Young's modulus value is quite similar to the one obtained from the CEB-FIP model code [8]. The stress at crack initiation, σ_I, is about the $f_{fctk,min}$ value

Fax: +351 253510217
E-mail: .epereira@civil.uminho.pt

(2.7 MPa) obtained from the CEB-FIP recommendations, and is quite distinct of the value resulting from the proposal of TC 162-TDF (σ_1=0.7 $f_{fctm,fl}$). The second branch of the trilinear $\sigma - w$ diagram is a "quasi-plateau", and the maximum crack width is around 3 mm. The average fracture energy is about 15 times the fracture energy expected for a plain concrete of an average strength equal to the f_{cm} obtained in the tested SFRSCC specimens (0.1 Nmm/mm^2). In previous research with "conventional" concrete reinforced with 30 kg/m^3 of the same fibres used in the present SFRSCC, the fracture energy of SFRC specimens of more than 28 days old was about 22 times higher than the G_f of the corresponding plain concrete specimens [12]. Due to the increase efficacy of the reinforcing fibre mechanisms with the concrete age, it is expectable that, at 28 days, the G_{ff}/G_f ratio of the SFRSCC will be similar to the ratio obtained for the SFRC.
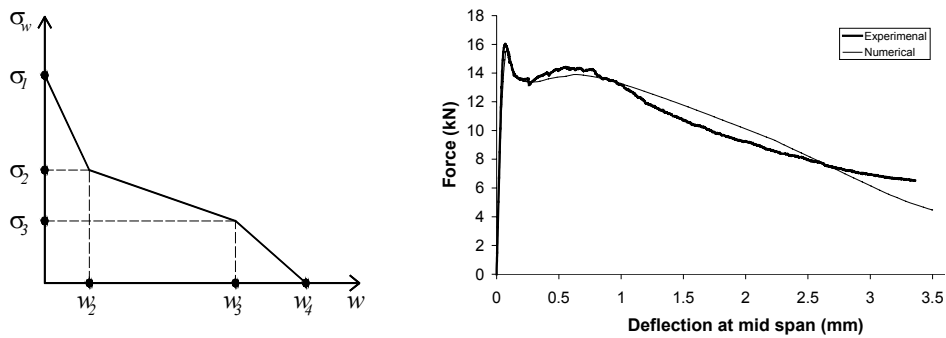

Fig. 8 – Stress-crack opening diagram.   Fig. 10 – Experimental vs. numerical curves

Table 3 - σ_i and w_i values for the conceived SFRSCC

Young's modulus [GPa]	σ_1 [MPa]	w_2 [mm]	σ_2 [MPa]	w_3 [mm]	σ_3 [MPa]	w_4 [mm]	err [%]	G_{ff} [Nmm/mm^2]
40.0	2.6	0.06	1.43	0.5	1.56	3	7.3	2.729

5. Conclusions

A rational strategy was developed to conceive selfcompacting steel fibre reinforced concrete (SFRSCC) not exceeding 410 kg/m^3 of cement content and having average compression strength greater than 50 MPa at 7 days. Furthermore, the equivalent flexural tensile strength for serviceability limit design is greater than 3 MPa at this age. To assure the selfcompacting requirements, fly ash, limestone filler and a third generation superplasticizer were used. The following three main steps compose the method proposed and employed in this work: definition of the binder paste composition; definition of the solid skeleton, where the fibres are included; definition of the binder paste content of the final composition.
The flexural behaviour was assessed carrying out three point bending notched beam tests according to the recommendations of TC 162-TDF. Using the force-deflection curves

Fax: +351 253510217
E-mail: .epereira@civil.uminho.pt

recorded from these tests, and performing an inverse analysis with a finite element computational code where crack initiation and crack propagation were simulated by interface finite elements, a trilinear stress-crack opening diagram, σ-w, was determined. This diagram is able to reproduce the post-peak behaviour of the conceived SFRSCC. According to the obtained σ-w diagram, the stress at crack initiation is smaller than the value recommended by TC 162-TDF. The first branch of the σ-w diagram has a very deep slope, followed by a "plateau" up to 0.5 mm. The energy dissipated in the fracturing process is about 15 times greater than the fracture energy expected for a plain concrete with an average strength equal to the f_{cm} obtained in the tested SFRSCC specimens.

Acknowledgments

References

1. Neville, A.M., 'Properties of concrete', ed. Sir Isaac Pitmann, London, (1963) 124 pgs.
2. Dewar, J. D., 'Computer Modelling of Concrete Mixtures', E & Spon, (1999).
3. Guazelli, E., Oger, L., 'Mobile Particulate Systems', **287** – NATO ASI Series, Netherlands, (1995).
4. Gomes, P.C.C., 'Optimization and characterization of high-strength self-compacting concrete', PhD thesis, UPC, Barcelona, Spain, (2002) 139 pgs.
5. Vandewalle, L. et al., 'Test and design methods for steel fibre reinforced concrete - Final Recommendation', Materials and Structures, 35(253), Nov. (2002) 579-582.
6. Vandewalle, L. et al., 'Test and design methods for steel fiber reinforced concrete. Recommendations for σ-ε design method', Materials and Structures, 33(226), Mar-Apr. (2000) 75-81.
7. Petersson, P.-E., 'Crack growth and development of fracture zones in plain concrete and similar materials', Lund Institute of Technology, Division of building materials, Report TVBM-1006 (1981).
8. CEB-FIP Model Code, Comite Euro-International du Beton, Bulletin d'Information nº **213/214** (1993).
9. Sena-Cruz, J.M., Barros, J.A.O., Fernances, A.R., Azevedo, A.F.M., Camões, A.F.F.L., 'Stress-crack opening relationship of enhanced performance concrete', 9th Portuguese Conference on Fracture (accepted to be published)
10. Azevedo, A.F.M.; Barros, J.A.O.; Sena-Cruz, J.M.; Gouveia, A.V., 'Software no ensino e no projecto de estruturas (Software in structural engineering education and design)', III Portuguese-Mozambican Conference of Engineering, August (2003) 81-92.
11. Schellekens, J.C.J., 'Interface elements in finite element analysis', TU-Delft report 25.2-90-5-17/TNO-IBBC report BI-90-165, October (1990).
12. Barros, J.A.O., Figueiras, J.A., 'Flexural behavior of steel fiber reinforced concrete: testing and modelling', Journal of Materials in Civil Engineering, ASCE, 11(4), (1999) 331-339.

Eduardo Pereira, Post cracking of selfcompacting steel, 10/10
Fax: +351 253510217
E-mail: .epereira@civil.uminho.pt